ELSEVIER

Journal of Nuclear Materials 251 (1997) 237–251

journal of nuclear materials

Defect interaction processes controlling the accumulation of defects produced by high energy recoils

M. Kiritani *

Department of Electronics, Hiroshima Institute of Technology, Miyake 2-1-1, Saeki-ku, Hiroshima 731-51, Japan

Abstract

Defect interaction processes involved in the microstructural evolution during irradiation with high energy recoils are discussed on the basis of experimental observations. First of all, an experimental procedure is outlined for identifying the nature of small defect clusters produced in cascades and subcascades. The procedure was the growth and shrinkage behavior of clusters produced in the cascades during subsequent irradiations with 1 MeV electrons in a high voltage electron microscope. It is shown that the analysis of the clusters produced during irradiation with high energy recoils can be used to identify the formation of sub-cascades. Various aspects of the one-dimensional glide of small self-interstitial atom (SIA) clusters and their role in defect accumulation are considered. The experimentally observed dose dependence of the cluster density is used to discuss the problem of fission–fusion correlation. Finally, some comments are made on the role of stochastic fluctuation of point defect reaction in the stability and lifetime of SIA clusters under cascade damage conditions.

1. Introduction

The evolution of defect microstructures during irradiation under cascade damage conditions is rather complicated and involves a variety of defect interaction processes. Furthermore, each of these processes is composed of several elementary processes. Thus in order to understand the observed final defect microstructure after a given irradiation experiment, it is necessary to establish a detailed understanding of different defect interaction processes involved in the evolution process. Only after such an understanding, it may become possible to predict the evolution of defect microstructure under a given new irradiation condition.

In the present paper, a number of defect interaction processes which are considered to be important under cascade damage conditions are identified. Consequences of these processes are discussed in terms of experimental observations. A recent progress in the experimental identification of the nature of small point defects clusters produced under cascade collision image is described. Particular emphasis is given to the one-dimensional motion of small SIA clusters produced in the cascades and its impact on the microstructural evolution during neutron irradiation.

2. Identification of the nature of small point defect clusters produced in collision cascades

Identification of the nature of small point defect clusters, clusters of vacancies or self-interstitial atoms (SIA), is the prerequisite for the progress of the investigation of defect structure evolution by irradiation with collision cascades. A powerful new technique has been introduced in which the identification is made from the behavior of clusters under electron irradiation in a high voltage electron-microscope.

2.1. Point defect reaction and expected behavior of small point defect clusters (produced in cascades) during electron irradiation

Electron irradiation produces the same number of single vacancies and isolated interstitials. Because of the higher mobility of interstitials, the reaction of interstitials

* Tel.: +81-82 921 3121 ext. 299; fax: +81-82 923 2679; e-mail: kiritani@ccsv.cc.it-hiroshima.ac.jp.

0022-3115/97/$17.00
PII S0022-3115(97)00278-X

dominates during the early state of the electron irradiation [1]. Even after the accumulation of vacancies, the motion-efficiency of interstitials, the product of the concentration and mobility of point defects, is at least that of vacancies. If SIAs are taken to react with defect clusters more strongly than vacancies, clusters of interstitials will be expected to grow and clusters of vacancies to shrink and disappear.

The method for identification stated above is logically very simple, but various precautions are required. First, the electron irradiation intensity in a high voltage electron microscope should not be too strong in order to avoid the formation of new point defect clusters. About one order of magnitude lower intensity than the strongest in a normal microscope is appropriate (strongest intensity obtainable is up to 10^{24} e/m^2 which produces point defects at the rate of 10^{-3}/s). The second is the temperature of electron irradiation. Lower temperature leads to the accumulation of more vacancies, which violates the interstitial dominant atmosphere. However, high temperatures should also be avoided to prevent the thermal annealing of defect clusters. The third is the influence of specimen surfaces, which is always accompanied with electron microscope irradiation. Both the prompt escape of interstitials to specimen surfaces and the accumulation of vacancies in the layers close to the surface should always be taken into account for the understanding of point defect behavior in thin foils and also at positions close to surfaces. Finally, though technical, because of the interest in the early stages of irradiation, the observation and recording with required resolution must be started immediately after the start of the irradiation, avoiding the drift motion of the sample. For this purpose, the area which had been observed in detail with a normal size electron microscope was brought to the electron beam path in a high-voltage electron microscope without mechanically moving the specimen (so called image shift technique).

2.2. Examination of neutron irradiation induced point defect clusters

The samples examined were irradiated with neutrons in three facilities: a fusion neutron source (RTNS-II), a fission reactor (JMTR) and a spallation neutron source (LASREF). Fig. 1 shows an example of the progressive

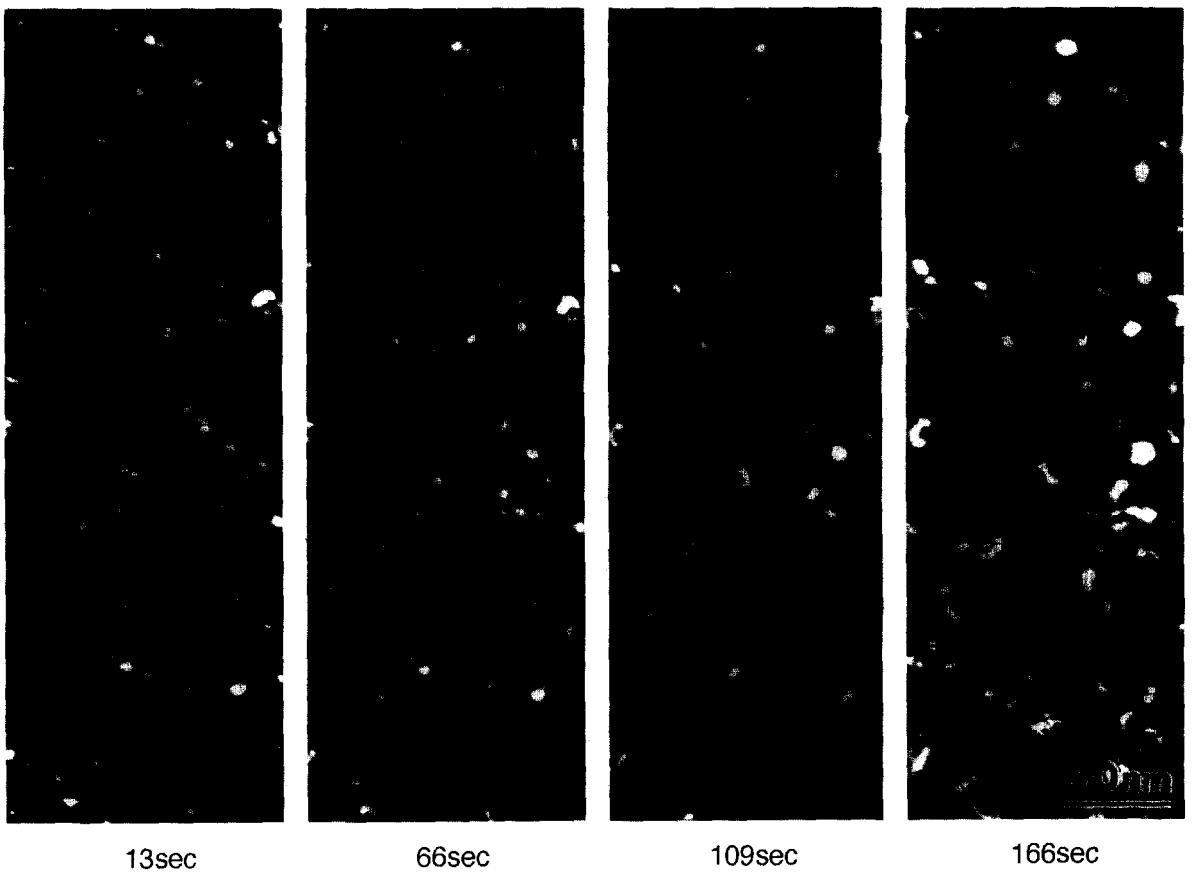

Fig. 1. Growth and shrinkage of neutron irradiation induced point defect clusters during electron irradiation in a high voltage electron microscope. Fe–16Ni–15Cr irradiated in JMTR as a thin foil up to 1.1×10^{24} n/m^2 at 353 K, and electron irradiated at 573 K with 1000 keV electrons with electron flux of 1.6×10^{24} e/m^{2}s.

Table 1
Point defect clusters introduced by neutron irradiation with three different facilities. Their nature was judged from their behavior under electron irradiation in a high voltage electron microscope

Material	Irradiation facility	Temperature (K)	Sample shape	Neutron dose ($/m^2$)	Vacancy clusters				Interstitial clusters			
					Number ($/m^2$)	Density (%)	Average size (nm)	V-concentration ($\times 10^{-5}$)	Number ($/m^2$)	Density (%)	Average size (nm)	V-concentration ($\times 10^{-5}$)
Cu	RTNS-II	300	Thin foil	1.5×10^{21}	1.4×10^{23}	97	1.8	4.2	4.9×10^{21}	3	4.0	1.3
			Bulk	5.0×10^{21}	2.7×10^{23}	84	0.9	1.9	5.3×10^{22}	16	4.9	21
	JMTR	300	Thin foil	6.2×10^{24}	1.9×10^{24}	99	1.6	45	8.5×10^{21}	<1	7.2	7.5
			Bulk	6.2×10^{24}	9.0×10^{23}	91	0.8	5.4	9.0×10^{22}	9	6.9	72
		473	Thin foil	3.0×10^{23}	1.5×10^{23}	99	2.7	10	1.6×10^{21}	1	8.0	1.7
			Bulk	3.0×10^{23}	5.0×10^{22}	91	2.6	3.2	5.0×10^{21}	9	8.8	6.6
	LASREF	317	Thin foil	1.5×10^{23}	2.5×10^{23}	99	2.4	13	2.0×10^{21}	1	7.1	1.7
			Bulk	1.5×10^{23}	1.8×10^{23}	92	1.8	5.5	1.5×10^{22}	8	8.3	17
Ni	RTNS-II	300	Bulk	2.0×10^{22}	2.3×10^{24}	79	1.9	8.1	6.0×10^{22}	21	3.8	3.8
	JMTR	330	Bulk	1.2×10^{22}	1.2×10^{24}	92	1.7	34	1.0×10^{23}	8	4.0	8.1
		573	Thin foil	3.7×10^{23}	1.1×10^{24}	92	1.4	23	1.0×10^{23}	8	14	51
Fe–16Ni–15Cr	JMTR	353	Bulk	1.1×10^{24}	4.7×10^{24}	93	1.0	50	3.5×10^{23}	7	2.0	26
		573	Thin foil[a]	1.0×10^{24}	3.7×10^{22}	77	2.0	1.5	1.1×10^{22}	23	3.0	1.9
			Thin foil[b]	1.0×10^{24}	3.8×10^{21}	26	8.0	2.5	1.1×10^{22}	74	10	21
		623	Bulk	1.1×10^{24}	–	0	–	–	1.4×10^{21}	100	8.0	1.7

[a] Thickness 20 nm.
[b] Thickness 120 nm.

change in the neutron-irradiation-induced point defect clusters in Fe–16Ni–15Cr (irradiated in JMTR) during electron irradiation. The majority of small defect clusters with white image contrast under weak-beam dark-field imaging condition are observed to shrink and disappear, and those with rather diffuse contrast grow and finally show the shape of dislocation loops. The former was judged to be point defect clusters of vacancy type, and the latter of interstitial type. Data on cluster density and sizes for three kinds of materials, copper [2], nickel [3] and the Fe–16Ni–15Cr alloy [4] irradiated in different facilities are shown in Table 1.

The present author performed neutron irradiations in various facilities and some heavy ion irradiations, and made analyses of the microstructure evolution mechanism during irradiation with collision cascades [5]. These analyses were on the experimental data of point defect clusters whose nature was judged from electron microscope images. The majority of vacancy clusters in fcc metals and alloys have the shape of stacking fault tetrahedra and they exhibit a sharp white triangle image when observed along the [110] direction with a proper weak beam dark field imaging condition. The image mainly comes from stacking faults of the tetrahedra, but not from the stair-rod dislocations [6]. The minimum size for the recognition of this shape is down to 1 nm, and the smaller ones were judged to be the same kind when the images belonged to the extrapolation from the larger size. On the other hand, dislocation loops are expected to exhibit the same image contrast regardless of their type, vacancy or interstitial, except for some details such as the inversion of the strong and faint contrast from their stacking fault on the same plane and also the inversion of inside–outside contrast of the loop dislocation between the two types, and the identification of the type from microscope images is impossible when the loop size is small (< 10 nm). At least, these loops can be discriminated from vacancy clusters in the shape of stacking fault tetrahedra. Small dislocation loops exhibit images of black dots with somewhat blurred periphery under bright field imaging condition, and the contrast becomes strong for small deviations from Bragg condition because the image comes from the strain-field of the dislocation, whereas the image of small stacking fault tetrahedra almost disappears under this condition. All the neutron irradiation-induced dislocation loops were found to grow under electron irradiation and were identified to be interstitial type. These dislocation loops have been inferred to be of the interstitial type from the variation with various irradiation parameters, and here it was confirmed that no major correction is necessary for the former data.

3. Concept of subcascades from the formation of point defect clusters

Splitting of a large collision cascades has been disclosed through the observation of vacancy clusters produced directly in the cascade core during irradiations which contain high energy primary recoils such as D–T fusion neutron irradiation [7,8]. In medium-atomic-weight metals such as Cu and Ni, those vacancy clusters (generally in the form of stacking fault tetrahedra) are isolated without directly exhibiting the formation of a great number of clusters from one high energy recoil. However, when the higher number density of vacancy clusters than the number of high energy recoils is considered, the splitting into subcascades is obvious. Simulation analyses with binary collision code were successfully made on subcascade configuration for these medium-atomic-weight metals [9,10], obtaining satisfactory agreement with the energy and separation distance of subcascades observed in experiments. On the other hand, in high-atomic-weight metals such as Ag and Au, vacancy clusters (also in the form of stacking fault tetrahedra) produced by the irradiation at some elevated temperature (~ 500 K) are much larger than those in medium-atomic-weight metals and their number density is reasonably understood from the number of high energy recoils [8]. Binary collision approximation simulation has also shown the absence of well defined separation into subcascades in these high-atomic-weight metals [9,10].

So far, the experimental observation of subcascade defects seems to be satisfactorily understood with the aid of binary collision approximation analyses. However, contrary to the statement above, the materials which had revealed their subcascades were heavy-atomic-weight metals, by the formation of closely spaced groups of vacancy clusters [7,8]. Even the recoil energy spectrum analysis of the observed vacancy cluster groups was possible to estimate the subcascade energy and the density of energy deposition [11]. Here, the formation of groups of small vacancy clusters are at lower temperatures (< 400 K for Ag and Au), and the clusters formed at elevated temperature are large isolated ones as described before. The aim of this section is to reconsider the concept of subcascades on the basis of the comparison of the results of the binary-collision-approximation simulations with that of the experimentally observed vacancy cluster formation, especially heavier-atomic-weight metals.

Firstly, the variation was examined of the spatial spread of collisions started from primary knock-on atoms (PKA) of the same energy. For example, 200 keV PKA in gold produces always approximately 4000 displaced atoms, but there is a wide variation in the degree of the localization of collisions. They are confined within a small volume of 10 000 atoms in some cases, but they are widely expanded to a large volume of 100 000 atoms in others. Towards the latter case of extreme, the number of separated localized volume of high collision density increases.

Secondly, the variation of collision distribution was examined with a collision density criterion. When a high value is assumed for the minimum collision density, several localized volumes are extracted, for example, up to 10 for the case of 200 keV PKA. When the minimum density

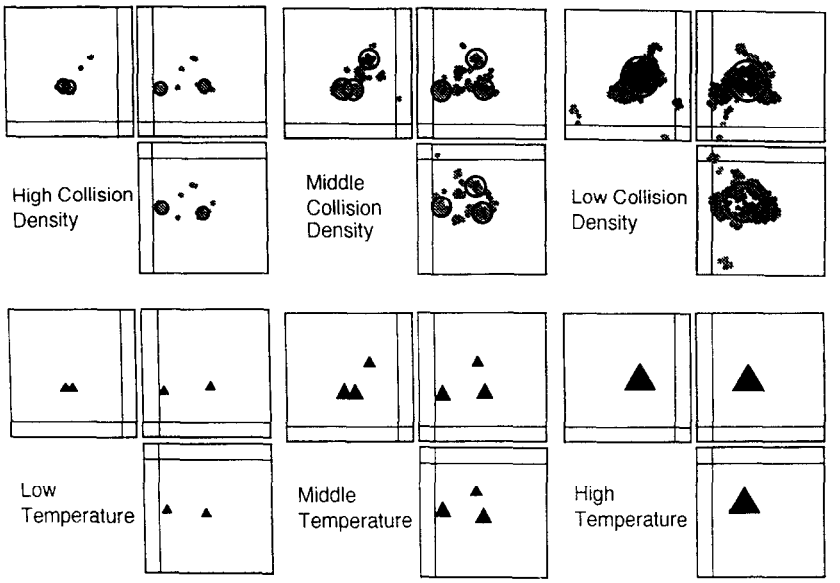

Fig. 2. Binary collision calculation for gold with PKA energy of 150 keV. Top row: Regions of collision density higher than three threshold values, from left to right 0.06, 0.05 and 0.04 dpa. Bottom row: Expected formation of vacancy clusters. Size of square: 15 nm.

is assumed at a lower value, all the collision zones are united to a continuous volume. Examples are shown in Fig. 2.

The consequence of the wide variation from the same energy of PKA corresponds to the wide variation of vacancy cluster groups in the monoenergetic heavy-ion irradiation [12]. The consequence of the variation with collision density criterion seems to correspond to the experimentally observed temperature dependence; a number of closely spaced small vacancy clusters at vacancy immobile low temperatures and a single large cluster at vacancy mobile high temperatures. especially in heavy-atomic-weight fcc metals [8].

Here, the splitting of a large collision cascade into subcascades should be defined depending on the kind of reactions after the collision. Subcascades in medium-atomic-weight materials such as Cu and Hi are well separated from each other and cannot cooperate with each other to form a vacancy cluster at a high temperature at which a subcascade cannot form a vacancy cluster. On the other hand, in heavy-atomic-weight materials such as Ag and Au small local high density collisions located very closely together can cooperate to form a larger cluster than at lower temperatures, even when they cannot form each of their own small clusters. Heavier materials behave as if they form subcascades at lower temperatures, but differently at higher temperatures.

4. One-dimensional motion of small interstitial clusters

In recent years the importance of small interstitial clusters has been recognized because of the strong possibility of their one-dimensional long range motion [13–15], for example, the elimination of interstitial clusters produced directly by collision cascades, which can be the origin of the so called 'production bias effect' [16,17]. One-dimensional motion of small clusters as small as several atoms has not been experimentally detected, except for those produced by the computer simulation with molecular dynamics [18]. On the other hand, motion of larger clusters (visible in electron microscope), clusters containing several tens of SIAs, has been detected and analyzed in detail, and their dynamical nature might be extrapolated to smaller sizes. In this section, observed behavior of small interstitial clusters is summarized, the damage microstructures which are believed to be the result of one-dimensional motion of interstitial clusters are quoted, and finally a remark is made on the tremendous difference in the reaction efficiency of interstitials between a one-dimensional and three-dimensional random walk with atomic distance jumps.

4.1. Detection and characteristics of the motion of visible small interstitial clusters

It has been long since the frequent motion of small interstitial clusters in metals was noticed during their formation under electron irradiation in a high voltage electron microscope [19–21]. The characteristics of the motion are summarized as follows.

(1) The analysis of the projected traces of the motion on microscope images showed the direction of motion to be along the most closely packed direction of atoms both in fcc and bcc metals (along [110] and [111]).

(2) The motion is not continuous but intermittent. As shown in Fig. 3, loops move while others stay at their position.

(3) The speed of motion is too high to be recorded and analyzed by a normal video recording (60 frames/s).

(4) A favorable circumstance for the motion of clusters is a continuous change of the size and distribution of surrounding clusters. Therefore the motion is more frequent during the growth of loops as shown in Fig. 4.

(5) Correlated motion is often observed, in which clusters move sequentially after the motion of other clusters nearby.

(6) A typical motion of small interstitial clusters is repeated back-and-forth motion between two positions. A loop stops when it comes very close to a neighboring loop, and therefore the length of back-and-forth motion is almost the separation distance between existing loops. The loop seems to stay some time at both ends, and often two loop images are observed because of the afterglow of the fluorescent screen of the microscope.

(7) Before the start of motion the microscope image of the cluster becomes faint as observed in Fig. 5, and the strong contrast recovers after the stop of its motion.

4.2. Proposal of the motion of groups of crowdions

Although the interstitial clusters of observable size are recognized to have the structure of dislocation loops in their stationary state, it is rather difficult to understand their one-dimensional motion in terms of conventional one-dimensional glide of dislocation in a force-field gradient. Dislocations on the facing two sides of a loop can move to the same direction with opposite signs of shear stress, and this cannot be expected for the small loops of the present interest. Or the difference in the shear stress of the same sign between the two segments is effective to move the loop as a whole, and the stress field gradient required for the motion becomes unrealistically high. Trinkaus et al. suggested a random 1D motion occurring by thermal activation [14,15].

The observed behavior of small interstitial clusters can be understood when one accepts a model of small interstitial clusters to have the structure which is composed of a group of [100] and [111] crowdions during its motion in fcc and bcc structure, respectively.

(1) Strong image contrast of a cluster when it is at a standstill is from the strain field of a normal dislocation

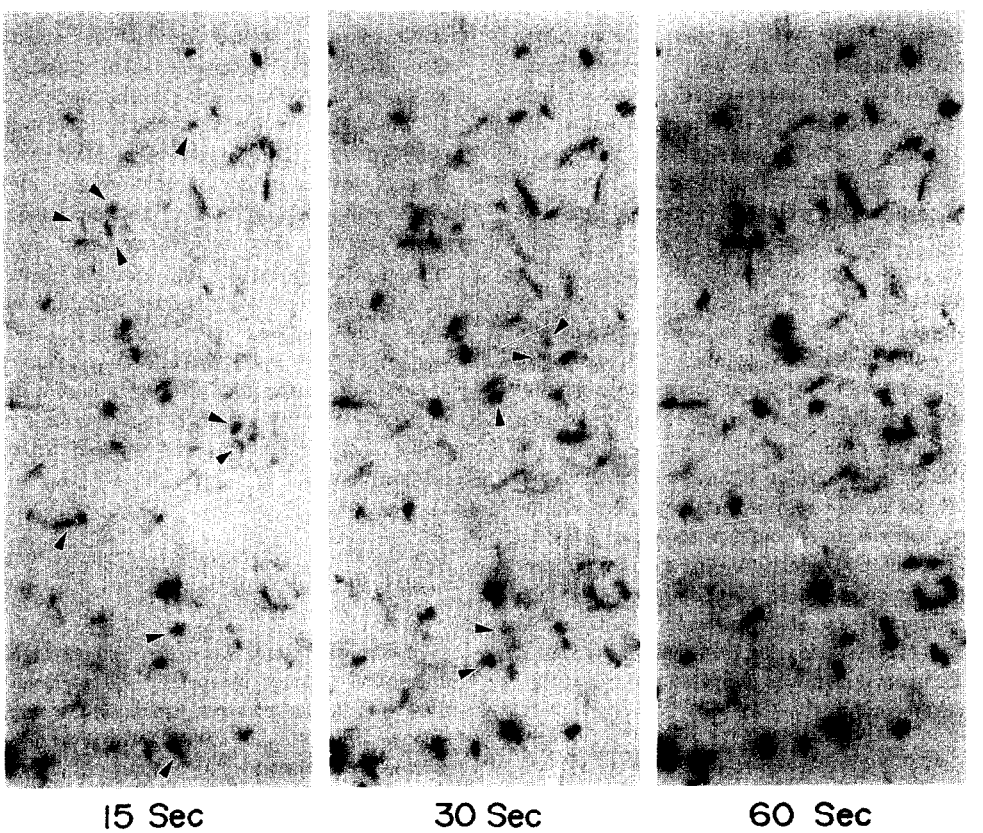

Fig. 3. Intermittent motion of small interstitial clusters observed during electron irradiation. Interstitial clusters pointed by arrowheads are observed to have moved in the next micrograph. Ni, 1000 keV, 5×10^{23} e/m^{2}s at 300 K.

loop, find the image becomes faint just before the start of its motion by expanding the localized strain of the dislocation to a wider range of crowdion structure.

(2) When we suppose a simple hexagonal shape of dislocation loop on (111) plane in fcc metals, two sets of facing segments can glide along the [110] direction on (111) planes together, but another set of facing segments can not be on normal glide planes when they want to move together. This difficulty does not exist for group crowdion motion.

(3) As stated before the dislocations of a loop move by shear stress and this cannot be expected for the present case of small loops. The bundle crowdion as a whole is understood as the center of compression strain, and the driving force for its motion is expected to come from the gradient of compression and expansion strain field. The back-and-forth motion in a narrow empty space between neighboring loops is made by the repulsive interaction between interstitial clusters with their compression strain field gradient.

(4) The glide motion of a normal dislocation is a type of motion under friction, but the motion of bundle crowdion is thought to be a type of motion with inertia. The bundle crowdion can be accelerated during its motion under strain field gradient and it can travel some distance after the gradient disappears or even after the sign of the gradient is reversed. This type of motion is the origin of the frequent observation of back-and-forth motion, and more generally important is the possibility of fairly long range motion of the group crowdion once it started.

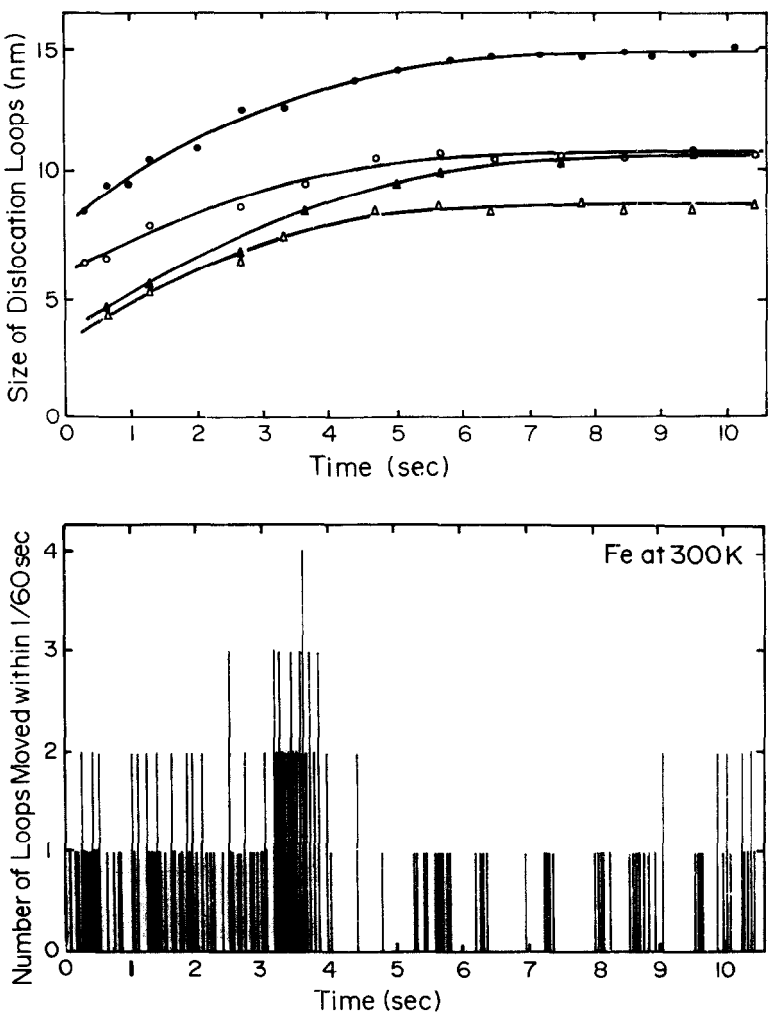

Fig. 4. Growth of interstitial clusters during electron irradiation of iron (top), and the frequency of their motion observed in an irradiated area of 100 μm^2 (bottom).

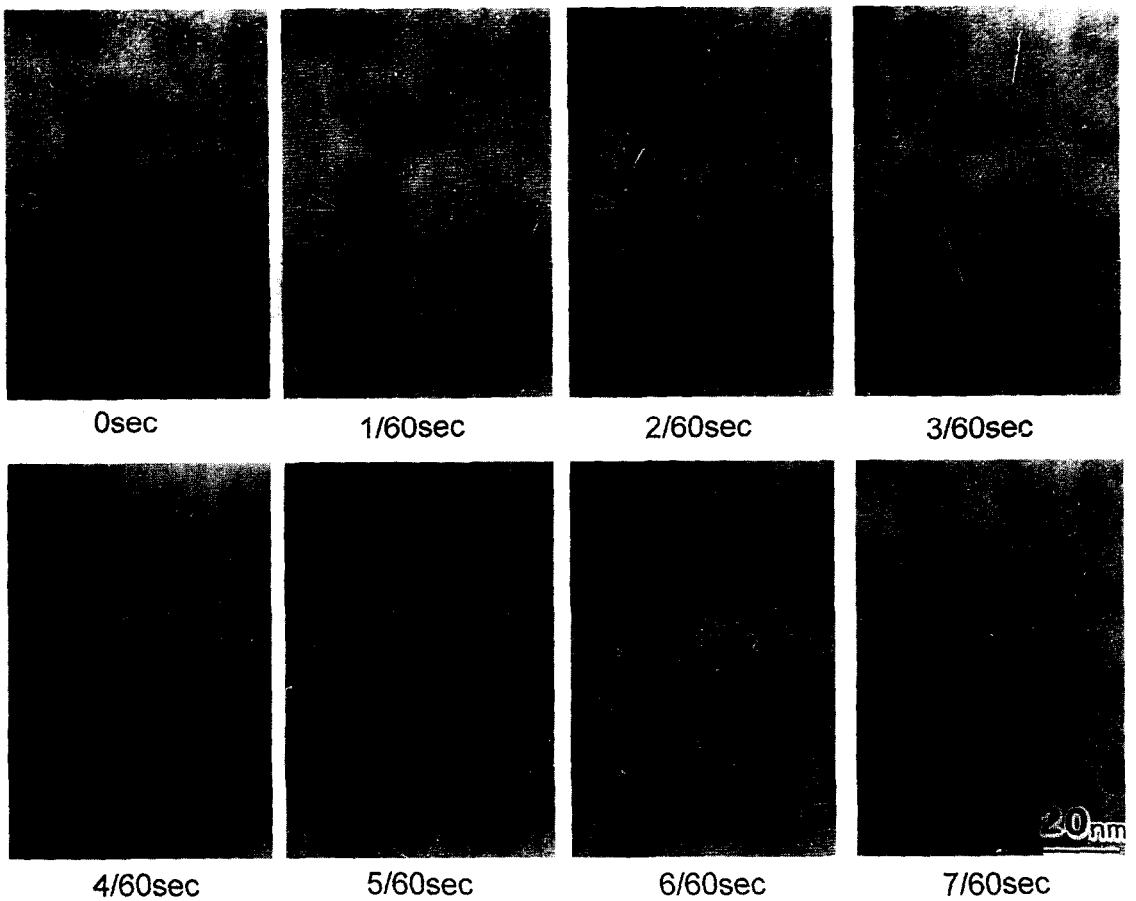

Fig. 5. Motion of small interstitial clusters during electron irradiation in iron. Note the change of image contrast before the start and after the finish of their motion.

Fig. 6. Difference in dislocation and void structures between two adjacent grains in a thin foil of Ni–2 at.% Cu irradiated with fission neutron to a fluence of 9×10^{23} n/m^2 (> 1 MeV) at 673 K.

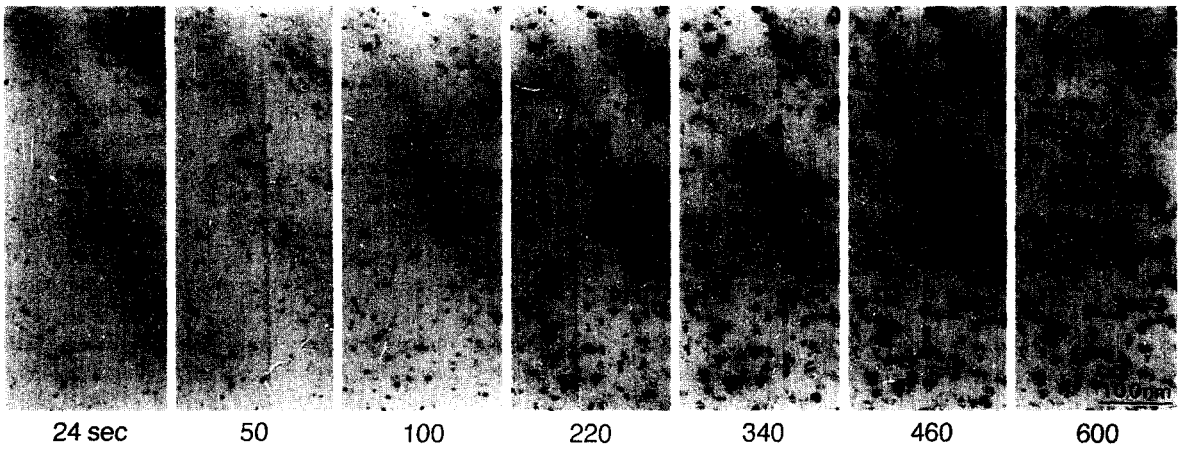

Fig. 7. Growth of neutron irradiation induced small point defect clusters in nickel to dislocation loops by electron irradiation in a high voltage electron microscope. Loops were identified after their growth to be interstitial type. Both neutron and electron irradiation at 473 K.

4.3. Consequence of one-dimensional motion of SIA clusters to the microstructure evolution during neutron irradiation

Many of the microstructures developed by collision cascade damage such as neutron irradiation, which have given us difficulty to understand with our conventional knowledge of point defect reaction, become easily understood when once the idea of the easy one-dimensional motion of small interstitial clusters is introduced.

4.3.1. Strong crystallographic orientation dependence

Although the penetration depth of neutrons through solid materials is so large, the irradiation of thin foils has been very efficiently utilized since the surfaces of thin foils provide well-defined efficient point defect sinks [13]. Experimental data on nascent microstructures from collision cascades without modification by freely migrating point defects have been obtained only from these thin foil irradiations. On the other hand, in these thin foil irradiations, crystallographic orientation dependence of damage

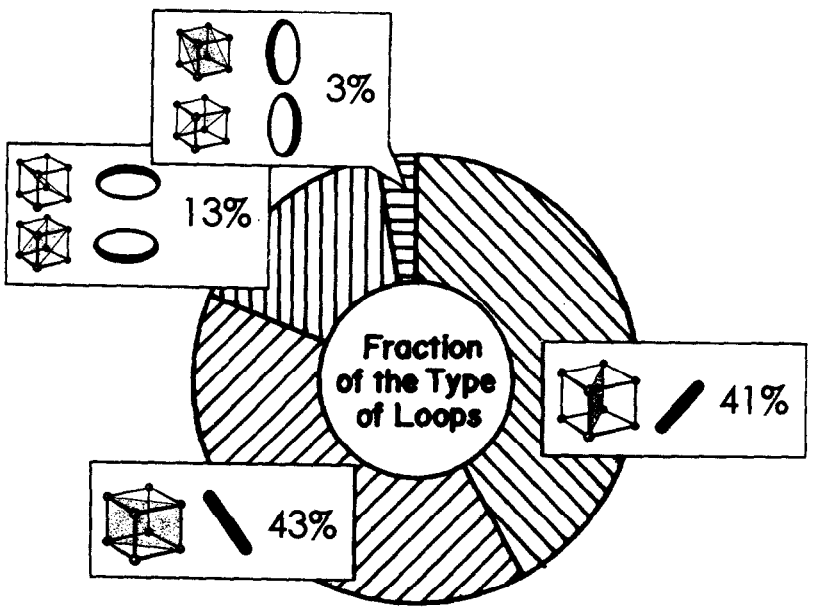

Fig. 8. Orientation of dislocation loops in neutron irradiated nickel examined after their growth by electron irradiation. Populations are not equal among equivalent crystallographic orientations.

accumulation shows up when the one-dimensional motion of interstitial clusters produced in collision cascades begins to play a role, even though crystallographic orientation dependence of the collision cascades themselves is not expected.

Fig. 6 is an example of very clear difference of defect structure evolution between adjacent crystal grains. Almost no dislocations but voids on the one side, and only dislocations developed from dislocation loops on the other. When the orientation of each grain was examined, all the [110] directions were found to have a steep angle with specimen surface in the former, but some were almost parallel to the specimen surface in the latter. All the small interstitial clusters produced in the cascades could escape to the surface before their growth in the former, but some stayed in the sample foil even when they have moved parallel to the specimen foil in the latter and developed into observable dislocation structures.

The above example is at a stage after some development of microstructures. At an early stage, the defect microstructure is composed of only small point defect clusters whose morphology cannot be analyzed in detail as it is. The efficient technique described in the first part of this paper to decorate defects by electron irradiation enables to analyze this early stage of defect structure development by neutron irradiation. Fig. 7 shows small dotted defects produced by neutron irradiation grow to dislocation loops by electron irradiation in a HVEM. Now the orientation of each loop, on which plane of the four (111) planes, can be recognized. The population of loops on four equiva-

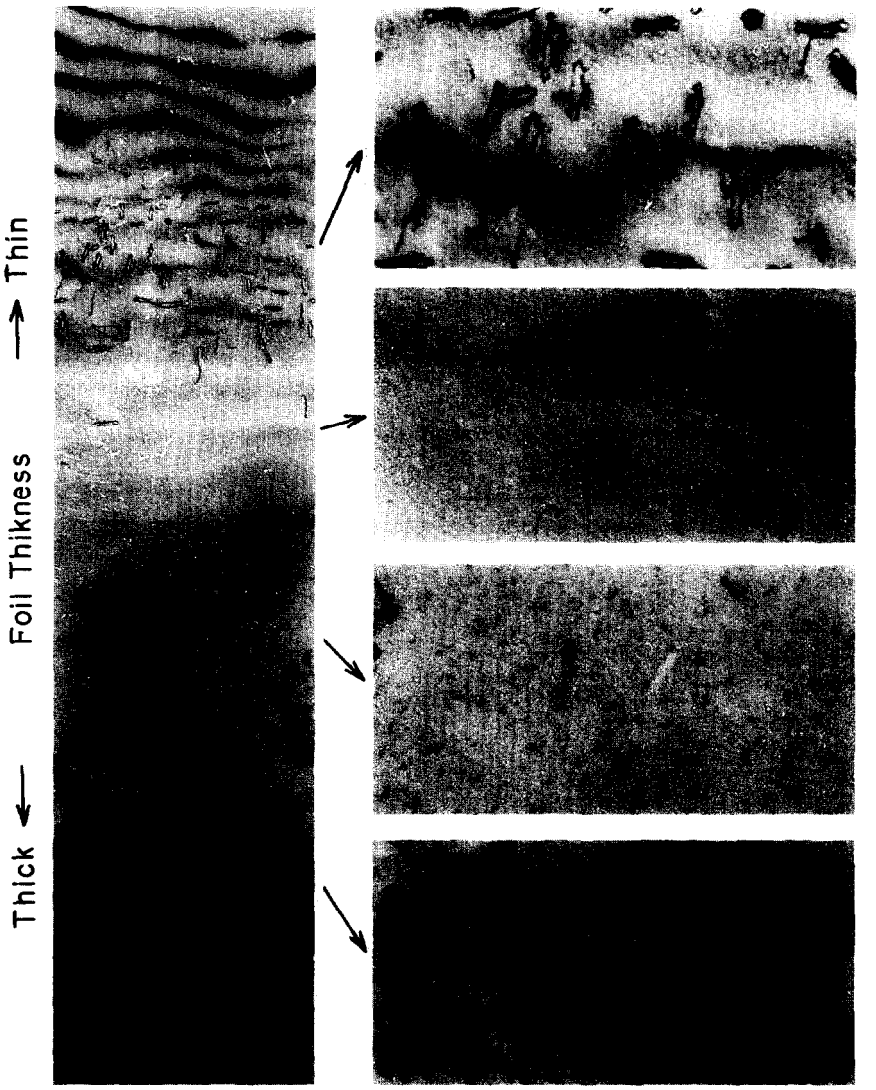

Fig. 9. Complex variation of defect microstructures with specimen foil thickness. Ni, 673 K up to 1×10^{24} n/m^2 at 673 K. From top (thinnest) to bottom (thickest): no defects, dislocation loops, no defects, voids, and dislocations developed from loops.

lent (111) planes was found to be significantly different: the population of loops was very low on those planes which had easy one-dimensional motion direction towards specimen surfaces as shown in Fig. 8.

4.3.2. Complex variation of defect microstructures with specimen thickness

The present author had several years of difficulty in understanding a complex variation in defect microstructure development with specimen thickness in neutron irradiated metals, which also differs from grain to grain even with the same thickness gradient. When the one-dimensional easy motion of small interstitial clusters was introduced, it became to be easily understandable.

Fig. 9 shows a typical example of a wedge shape specimen in which the thickness gradually increases from top to bottom of the figure. Five stages of the variation of defect microstructures are recognized.

(1) In the thinnest part, no defect structures developed because of the escape of all the freely migrating point defects to specimen surfaces.

(2) In a more thicker part, dislocation loops have grown to appreciable size. The repulsive interaction between loops during early stages of irradiation is thought not to be enough to send all the clusters to specimen surfaces even with the one-dimensional motion.

(3) In a medium thick part of the sample shown here, no defect microstructure was seen to evolve. The thickness is thought to be appropriate to produce a sufficient number of dislocation loops to have mutual repulsive interaction and the surfaces are close enough for their sinks.

(4) In the thicker part of the foil, high density of small voids but no dislocations were observed. Interstitial clusters could escape by one-dimensional motion to surfaces, and the thickness is now enough to accumulate vacancies.

(5) In the thickest part in the figure, dislocation structures developed from interstitial clusters. Surfaces were too far to be reached by all the interstitials and there was enough supply of freely migrating interstitials.

4.3.3. Enhanced formation of interstitial clusters near dislocations

Enhanced formation of interstitial clusters, as shown in Fig. 10, on the dilatation strain side of an edge dislocation is frequently observed under neutron irradiations where the formation of interstitial clusters in the dislocation free matrix is very low [22,23]. This type of defect microstructure has never been observed by electron irradiation, and is thought to be characteristic of cascade damage. In the case of electron irradiation, defect microstructures looking similar to the case of neutron irradiation are produced, but with the cluster of vacancies on the compression side of edge

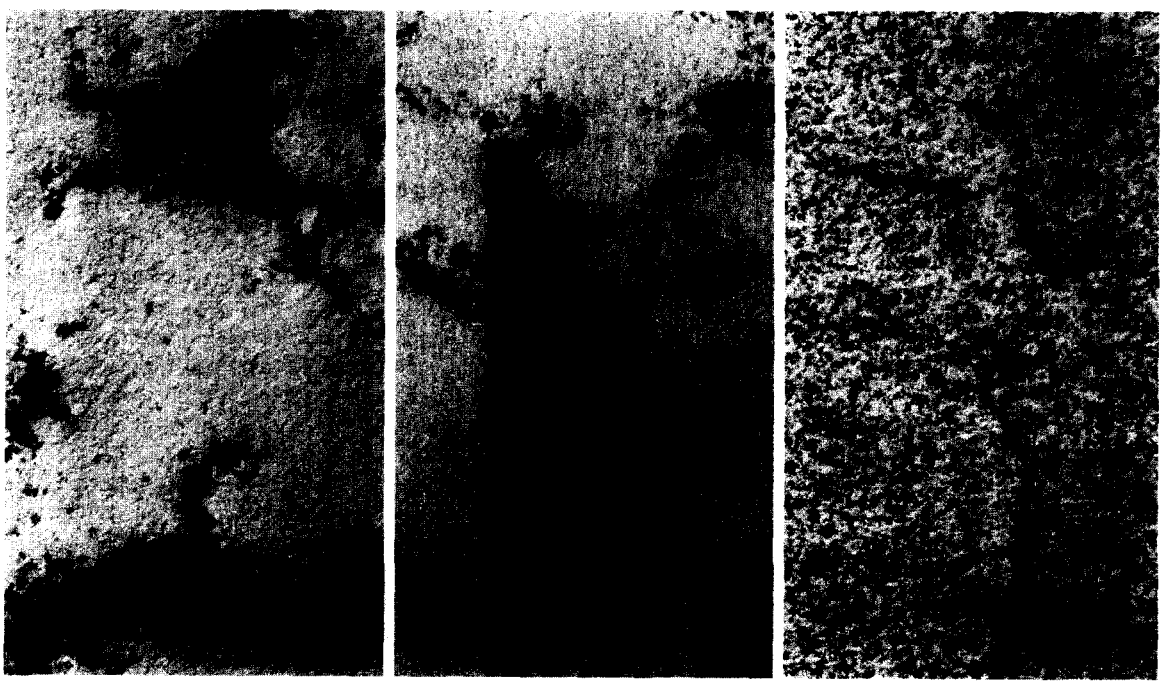

Fig. 10. Comparison of the formation of dislocation loops in the vicinity of pre-existent dislocations in copper and copper dilute alloys irradiated as bulk, 2.5×10^{22} n/m^2 at 473 K.

dislocations. These vacancy clusters are understood to have been formed from locally enriched vacancies resulting from the efficient escape of interstitials due to repulsive interaction with the dislocation.

A very high nucleation rate of interstitial clusters near dislocation, even the smaller nucleation rate in a dislocation free matrix, cannot be expected from the well known point defect production rate dependence of the nucleation rate of the same type of clusters under homogeneous introduction of point defects by electron irradiation [24,25]. They are obviously related to the direct production of interstitial clusters from collision cascades. However, at present, the extent of contribution of the one-dimensional motion of interstitial clusters to enhance the formation near dislocation is not well understood.

4.4. Efficiency of reaction with sinks during one-dimensional motion

So far the discussions have been made to understand each specific defect microstructure development, but the general importance is in the difference of the point defect reaction under different diffusion modes. A detailed analysis on the impact of one-dimensional interstitial cluster motion has been given recently by Trinkaus and others, predicting the consequence to the final microstructural development [14,15]. The purpose of the analysis in this section with a highly simplified model is intending to illustrate the basic concept of the difference in the efficiency of the reaction with sinks by the difference in the diffusion mode. The number of atomic sites through which a point defect or a point defect cluster travels until it reaches at point defect sinks will be examined.

When the mean free path distance of the one-dimensional motion λ is n times the atomic distance a, $\lambda = na$, where a is the atomic distance, and the distance to the sink is L, the number of one-dimensional motion required to reach the sink is approximately $(L/\lambda)^2$, if the direction of the motion is randomly changed at each step. The number of atomic sites traced during this diffusion is

$$N_{GC} = (L/\lambda)^2 n = (L/a)^2 (1/n). \quad (1)$$

On the other hand, if the diffusion is carried out with a normal random walk with an atomic distance jump, the number of atomic sites traced by a diffusion element is simply

$$N_{RW} = (L/a)^2. \quad (2)$$

It is natural to suppose the reaction of a point defect is proportional to the atomic sites it traces during its diffusion, and the efficiency ε_{GC} of reaction for one-dimensional motion relative to the atomic distance random walk is simply

$$\varepsilon_{GC} = N_{GC}/N_{RW} = 1/n. \quad (3)$$

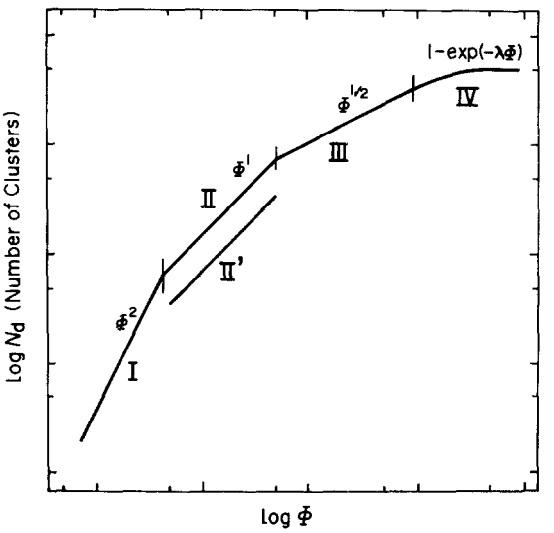

Fig. 11. Progressive variation of the accumulation mode of vacancy clusters produced by irradiation damage with collision cascades. The appearance of the stages depends on the irradiation condition.

This means a remarkable decrease of reaction efficiency for longer mean free path of one-dimensional motion, and has all the variety of important consequences during damage microstructure evolution. Interstitials, if they make one-dimensional motion, may reach sinks at distance without making a reaction during their diffusion. On the other hand, vacancies, if they make a random walk, have much more chance to make a reaction and disappear during diffusion before they reach the same geometry of sinks.

5. Defect accumulation mode and fission–fusion correlation

5.1. Progressive variation of defect accumulation mode

Surveying defect structure development under various irradiation conditions by fission and fusion neutrons and light and heavy ions, the present author organized the accumulation mode of vacancy clusters produced directly from collision cascades as shown in Fig. 11 [21].

Stage I: During the very beginning of irradiation at vacancy immobile low temperatures, the number of vacancy clusters increases proportionally to the square of irradiation dose. This stage is understood as the formation of microscopically visible clusters from high density of vacancies produced by preceding cascade collision with an aid of some impact effect from another cascade collision in a close distance [11].

Stage II: The simplest case of the proportional increase of vacancy clusters with irradiation dose, realized only when the influence of the reaction of freely migrating

interstitials is strictly avoided such as the irradiation of thin foils with neutrons and the heavy ion irradiation with not too high energy to have shallow penetration depth. Defects directly produced from collision cascades are most appropriately extracted from this stage.

Stage II′: The same proportional increase with irradiation dose as in stage II, but with a lower level of vacancy cluster density. This is the case of a low sink (permanent) density which allows the continuous formation of interstitial clusters and a part of freely migrating interstitials continuously eliminates the vacancy clusters [26].

Stage III: The number of vacancy clusters increases proportionally to the square-root of irradiation dose. This is the case of the combination of a low permanent sink strength/density and no interstitial cluster formation, typically well annealed samples at elevated temperatures. Freely migrating interstitials are shared between fixed sinks and increasing vacancy clusters, and they slow down the accumulation [26,27].

Stage IV: Exponential approach to a fixed level of the number density of vacancy clusters. This stage is realized by the geometrical overlap of the defects produced by cascades with existing high density of defects in the case of efficient elimination of freely migrating point defects to permanent sinks. Very thin foil irradiation with neutrons and heavy ion irradiation very close to the specimen surface belong to this case [27].

Here it should be noticed that some of the stages appear as sequence, but generally they do not, depending on the kind of material, irradiation conditions such as specimen geometry, irradiation temperature, and irradiation dose.

5.2. *Fission–fusion neutron irradiation correlation*

When one is involved in the research on the neutron irradiation effect for the development of fusion reactor materials, at present he has to rely on the irradiation with fission reactors. He should know how to convert the data from fission reactor irradiation to those under fusion neutron irradiation environment, so called 'fission–fusion neutron irradiation correlation'. The present author reported the result of direct comparison of defect structure evolution between the two, though limited to very low dose irradiation [28], but they were not satisfactory. Some systematic data were there for fusion neutron irradiation for which the mode of defect accumulation were known, but on the other hand only a single data point was available for fission reactor irradiation with which one cannot tell whether it belongs to the same mode of defect accumulation.

Recently, the development of Multi-Section-Removable-Irradiation-Rig in JMTR enabled to obtain systematic data along a series of irradiation doses under consistent irradiation field with a good temperature control [29]. Fig. 12 is an example of comparison of the accumulation of

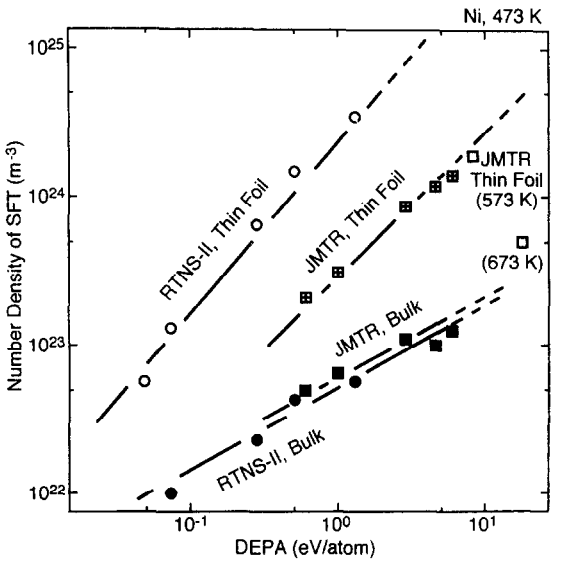

Fig. 12. Comparison of the accumulation modes of vacancy clusters between D–T fusion neutron irradiation (RTNS-II) and fission reactor irradiation (JMTR). Ni at 473 K.

vacancy clusters in nickel between fission reactor (JMTR) neutron irradiation and D–T fusion neutron irradiation (RTNS-II). Astonishingly, the accumulation in bulk samples coincides very well, the accumulation mode even with the same absolute level, when scaled along DEPA (damage energy per atom unit) which is the parallel scaling as conventional dpa unit but without including the assumption of threshold energy for displacement damage. However, this coincidence should be regarded fortuitous when the existence of such a large difference in thin foil samples is known. This difference and similarity means that defects produced directly from collision cascades are so much different between the two but the reaction of freely migrating defects fortuitously brought to the same level. Here at least, the kind of defect reaction in bulk is the same, but the parameters included should be very different, and therefore there is no proof for the coincidence when the accumulation modes goes into different stages. Further investigation is needed before a general understanding of defect accumulation mechanism and fission–fusion correlation is obtained.

6. Remarks on other component processes

6.1. *Consequence of stochastic fluctuation of point defect reaction*

The position of collision with incident energetic particles is random, and the diffusion path of point defects produced by the collision is also random. This randomness is spatial as well as temporal when one considers the

reaction of point defects at a fixed position. It seems to be worthwhile to note that the progress in the experimental technique is reaching the level of direct detection of these stochastic random reactions [29,30].

Here it should be emphasized that the randomness is remarkably different from homogeneity. Inhomogeneity is one of the prominent characteristics of randomness. When the point defect reaction is averaged over a large volume or a long time period, the amount of reaction is uniquely defined. However, when one is concerned with a small volume or a short time period, the deviation from the average becomes not negligible. This deviation is particularly important in the balanced system of vacancies and interstitials, because there is a definite chance of predominance of one species of point defects over the others.

By a large collision cascade in metals, a large vacancy cluster is formed at the center of the cascade collision and higher numbers of smaller interstitial clusters are expected to be formed surrounding the cascade core. However, the finally observed number of interstitial clusters is generally much less than those of vacancy clusters as in Section 2 of this paper. The reason for the very small survival ratio of interstitial clusters may be partly attributed to the fluctuation of point defect reaction, the absorption of more vacancies than interstitials when the cluster is still small. The positional instability of small interstitial clusters may be another reason, and the comparison of the two reasons is a future problem to be solved.

6.2. Atomistic process of interstitial cluster growth during irradiation

The simplest case of the growth of interstitial clusters in the form of dislocation loops during irradiation is a constant speed growth under the balanced condition of vacancies and interstitials [31]. The constant speed in linear scale (not the area of loop or the number of interstitials in a loop) has been understood from the linear increase of the absorption site of point defects along the dislocation line.

Recent progress in the observation technique enabled to analyze the growth of a faulted loop with almost atomic scale resolution. Angular (typically hexagonal) shape interstitial type dislocation loops were found to start their growth by absorbing an interstitial atom at its corner followed by a prompt propagation of the atomic step along the straight line. The reason for the preferential absorption at the corner rather than on the line of dislocation is sought in the strong attractive flow of interstitials toward the corner along the dilatational strain field gradient [32]. The constant speed of the growth is naturally kept because of the fixed number of corners on a loop. Now the kinetics type of formulation of the accumulation of defects as dislocation loops are not altered, but the absolute speed is much different from the case of the absorption of interstitials along the dislocation line of the loop.

6.3. Role of vacancies released from collision cascades

Freely migrating point defects, especially during irradiation with collision cascades, are composed of point defects with two different histories; the first point defects are isolated point defects from their birth by collision and the second point defects are released from point defect clusters once formed directly from collision cascades. Although their role in microstructure evolution is similar as each point defect reacts irrespective of their history, they should be discriminated from each other as component processes during the damage microstructure development because their role might be different depending on the stage they take part in.

For the kind of stainless steel Fe–16Ni–15Cr, in which well separated vacancy clusters are formed from subcascades, the size distribution of the clusters was compared between those introduced by the irradiation at an elevated temperature and those after the annealing up to the same elevated temperature after the introduction by the irradiation at a lower temperature [33]. Survived clusters after annealing were found to distribute at much smaller sizes than those directly formed at that temperature, and this indicated that the smaller size of clusters was not formed from the beginning at the elevated temperature.

Let us consider the formation of a single large vacancy cluster in heavier metals such as Ag and Au at elevated temperatures [7], which was partly discussed in Section 3 of this paper. It is not clear at present whether small vacancy clusters are formed once from the subcascade type of concentrated vacancies before they evaporate and cooperate to form single larger clusters later. If the reaction process found in Fe–16Ni–15Cr is allowed to be adopted to these heavier metals, vacancies formed in several localized volumes by collisions directly cooperate to form a single large cluster without going through the formation of smaller clusters.

On the other hand, vacancies released from their clusters play an important role in some cases. As observed in Section 2 in this paper, the formation of vacancy clusters from collision cascades is more abundant at lower temperatures. When the irradiation temperature is raised to a higher temperature after the low temperature irradiation, vacancies released from these small clusters can eliminate existing interstitial clusters and consequently suppress the development of dislocation structure during the higher temperature irradiation. This has been proposed as one of the mechanisms of the suppression of microstructural evolution in temperature cycle irradiation [34]. Systematic date on the thermal stability of small vacancy clusters are now available from the annealing experiment of various sizes of vacancy clusters introduced by electron irradiation in a high voltage electron microscope, and quantitative analyses of the role of released vacancies in the microstructure evolution during neutron irradiation are now in progress for a number of metals and alloys [33,35].

Acknowledgements

The present author is grateful to his co-workers including graduate students for the use of unpublished results. They are Drs, Mr and Mrs S. Arai (2, 4, 6.1, 6.2), K. Arakawa (6.1, 6.2), M. Horiki ((2, 6.3), E. Iiyoshi (3), Y. Kizuka (2, 3), T. Kouchi (4), Y. Ogasawara (2, 5.2, 6.3), Y. Satoh (2, 4, 5.2) and K. Satori (4). The numbers in parentheses are the numbers of sections to which they contributed.

References

[1] M. Kiritani, Ultramicroscopy 29 (1991) 135.
[2] Y. Kizuka, Y. Satoh, S. Arai, M. Kiritani, to be published in Philos. Mag.
[3] Y. Ogasawara, Y. Satoh, S. Arai, M. Kiritani, Radiat. Eff. Defects Solids 139 (1996) 287.
[4] M. Horiki, Y. Satoh, S. Arai, M. Kiritani, to be published in J. Nucl. Mater.
[5] M. Kiritani, J. Nucl. Mater. 216 (1994) 220.
[6] Y. Satoh, H. Taoka, S. Kojima, T. Yoshiie, M. Kiritani, Philos. Mag. A70 (1994) 869.
[7] M. Kiritani, J. Nucl. Mater. 137 (1986) 261.
[8] M. Kiritani, J. Nucl. Mater. 155–157 (1988) 113.
[9] H.L. Heinisch, B.N. Singh, Philos. Mag. A67 (1993) 407.
[10] Y. Satoh, S. Kojima, T. Yoshiie, M. Kiritani, J. Nucl. Mater. 179–181 (1991) 901.
[11] M. Kiritani, T. Yoshiie, S. Kojima, Y. Satoh, Radiat. Eff. Defects Solids 113 (1990) 75.
[12] M. Kiritani, J. Nucl. Mater. 191–194 (1992) 1128.
[13] A.J.E. Forman, C.A. English, W.J. Phythian, Philos. Mag. A66 (1992) 655.
[14] H. Trinkaus, B.N. Singh, A.J.E. Forman, J. Nucl. Mater. 199 (1992) 1.
[15] H. Trinkaus, B.N. Singh, A.J.E. Forman, J. Nucl. Mater. 206 (1993) 200.
[16] C.H. Woo, B.N. Singh, Phys. Status Solidi B159 (1990) 609.
[17] C.H. Woo, B.N. Singh, Philos. Mag. A65 (1992) 889.
[18] Y. Shimomura, R. Nishiguchi, T.D. de la Rubia, M.W. Guinan, Radiat. Eff. Defects Solids 130&131 (1994) 434.
[19] K.H. Westmacott, A.C. Roberts, R.S. Barnes, Philos. Mag. 7 (1962) 2035.
[20] M. Kiritani, Proc. Int. Conf. High Voltage Electron Microscopy, Antwerp, 1980, p. 196.
[21] M. Kiritani, J. Nucl. Mater. 206 (1993) 156.
[22] Y. Satoh, I. Ishida, T. Yoshiie, M. Kiritani, J. Nucl. Mater. 155–157 (1988) 443.
[23] S. Kojima, T. Yoshiie, M. Kiritani, J. Nucl. Mater. 155–157 (1988) 1249.
[24] N. Yoshida, M. Kiritani, J. Phys. Soc. Jpn. 35 (1973) 1418.
[25] M. Kiritani, H. Takata, J. Nucl. Mater. 69&70 (1978) 277.
[26] M. Kiritani, Mater. Sci. Forum 15–18 (1987) 1023.
[27] M. Kiritani, Y. Fukuta, T. Mima, E. Iiyoshi, Y. Kizuka, S. Kojima, N. Matsunami, J. Nucl. Mater. 212–215 (1994) 192.
[28] M. Kiritani, T. Yoshiie, S. Kojima, Y. Satoh, K. Hamada, J. Nucl. Mater. 174 (1990) 327.
[29] T. Yoshiie, M. Kiritani, Mater. Sci. Forum 15–18 (1987) 889.
[30] K. Arakawa, K. Satori, S. Arai, M. Kiritani, Trans. Mater. Res. Soc. Jpn. 16A (1994) 365.
[31] M. Kiritani, N. Yoshida, H. Takata, Y. Maehara, J. Phys. Soc. Jpn. 38 (1975) 1677.
[32] M. Kiritani, N. Yoshida, H. Takata, J. Phys. Soc. Jpn. 35 (1973) 306.
[33] M. Horiki, M. Kiritani, J. Nucl. Mater. 239 (1996) 34.
[34] M. Kiritani, T. Yoshiie, M. Iseki, S. Kojima, K. Hamada, M. Horiki, Y. Kizuka, H. Inoue, T. Tada, Y. Ogasawara, J. Nucl. Mater. 212–215 (1994) 241.
[35] Y. Ogasawara, M. Kiritani, to be published in J. Nucl. Mater.